processes

MDPI

Article

Efficient Removal of Cr (VI) with Biochar and Optimized Parameters by Response Surface Methodology

Hao Peng *, Jing Guo, Hongzhi Qiu, Caiqiong Wang, Chenyu Zhang, Zhihui Hao, Yating Rao and Yanhong Gong

Chongqing Key Laboratory of Inorganic Special Functional Materials, College of Chemistry and Chemical Engineering, Yangtze Normal University, Chongqing 408100, China; 20171110@yznu.edu.cn (J.G.); q780173781@126.com (H.Q.); wcq18290390314@163.com (C.W.); hzh3229224722@126.com (C.Z.); zcy20010126@126.com (Z.H.); rytlill@163.com (Y.R.); scarlett20001212@163.com (Y.G.)

* Correspondence: penghao@yznu.edu.cn

Abstract: A highly efficient reduction process of Cr (VI) with biochar was conducted in this paper. The results showed that nearly 100% Cr (VI) was reduced at selected reaction conditions: Dosage of biochar at m (C)/m(Cr) = 3.0, reaction temperature of 90 °C, reaction time of60 min, and concentration of H_2SO_4 of 20 g/L. The reduction kinetics analysis demonstrated that the reduction of Cr (VI) fitted well with the pseudo-first-order model and the apparent activation energy was calculated to be 40.24 kJ/mol. Response surface methodology confirmed that all of the experimental parameters had a positive effect on the reduction of Cr (VI). The influence of each parameter on the reduction process followed the order: Dosage of biochar>concentration of H_2SO_4>reaction temperature >reaction time. This paper provides a versatile strategy for the treatment of wastewater containing Cr (VI) and shows a bright tomorrow for wastewater treatment.

Keywords: chromium; response surface methodology; reduction; biochar

Citation: Peng, H.; Guo, J.; Qiu, H.; Wang, C.; Zhang, C.; Hao, Z.; Rao, Y.; Gong, Y. Efficient Removal of Cr (VI) with Biochar and Optimized Parameters by Response Surface Methodology. *Processes* **2021**, *9*, 889. https://doi.org/10.3390/pr9050889

Academic Editors: Maria Jose Martin de Vidales and Bipro R. Dhar

Received: 1 April 2021
Accepted: 13 May 2021
Published: 18 May 2021

1. Introduction

Chromium pollution is a serious environmental problem and Cr (VI) has been classified in Group 1 by the IARC (International Agency for Research on Cancer) [1–5]. Cr (VI) has many negative impacts on earthworms, plants, fish, and other lives. It increases the reproduction and mortality of earthworms, and is toxic on the kidneys and cells of animals and humans, etc. In the earth, chromium mainly exists in the oxidative states of hexavalent and trivalent chromium. Chromium (III) compounds are relatively stable and have low solubility and mobility. In contrast, chromium (VI) mainly exists as chromate (CrO_4^{2-}, $HCrO_4^-$) and dichromate ($Cr_2O_7^{2-}$), which have high solubility. In recent years, many technologies had been applied to treat wastewater containing Cr (VI) [6].

Physicochemical technologies (such as ion exchange, membrane filtrate, and chemical precipitation) are easy to employ with high removal efficiency [7–10]. The so-called electrochemical technology associated with electricity shows high removal efficiency and is clean and environmentally friendly [11–13]. Photocatalysis and nanotechnology have also been developed for the treatment of wastewater and show great performance [14,15]. Meanwhile, problems such as large-scale application, secondary pollution, and high cost remain. Therefore, it is urgent to develop useful technologies for Cr (VI) treatment [16–18]. Recently, the reduction of Cr (VI) to Cr (III) has attracted much more attention [12,13,19–21]. The reduction process of Cr (VI) with oxalic acid with and without Mn (II) has been investigated and the results showed that Cr (VI) could not be reduced in an oxalic acid solution or an Mn (II) solution, while nearly 99% of Cr (VI) reduced to Cr (III) in an oxalic acid solution mixed with Mn (II). Thus, it was concluded that Mn (II) can catalyze the reduction process of Cr (VI) with oxalic acid. Many methods had been developed to promote the reduction process of Cr (VI) with oxalic acid, such as catalyzation by TiO_2, Al_2O_3, FeOOH, and

sunlight, but these methods are still not easily used for practical applications, especially in groundwater remediation.

Biochar derived from plant and animal wastes is a typical adsorbent to remove inorganic and organic pollutants in water due to its low cost and abundant feed stock availability [22–24]. In addition, the large surface area, high mineral content, and rich oxygen-containing functional groups of biochar are favorable for the adsorption of wastewater contaminants such as antibiotics, dyes, and heavy metals [25–27]. The quality and yield of biochar are greatly affected by the hemicellulose, lignin, and cellulose contents of feedstock, as well as the moisture content. The cellulose, hemicellulose, and lignin contents of sugarcane bagasse is, respectively, 38–59%, 18–26%, and 16–25%, which might allow to obtain a high biochar yield due to its high lignin content. In this paper, biochar was applied to adsorb chromium (VI); after conducting the experiments, the biochar actually acted as a reductant and the chromium (VI) was reduced by biochar rather than just adsorbed by it—that is to say, the imaginative adsorption process proved to be a reduction process. The impact of the experimental parameters, including the dosage of biochar, reaction temperature, reaction time, and concentration of H_2SO_4, on the reduction process were investigated. Moreover, reduction kinetics analysis was conducted.

2. Materials and Methods

2.1. Materials

$K_2Cr_2O_7$, H_2SO_4, and biochar were of analytical grade and used as received without further purification, which were purchased from Kelong Co., Ltd., Chengdu, China. All solutions were prepared with deionized water with a resistivity greater than 18 MΩ/cm (HMC-WS10) [12,13,19,28].

2.2. Experimental Procedure

All of the experiments were conducted in a beaker placed in a thermostatic water bath with a temperature precision of ±0.1 °C [12,13]. In the batch experiments, the Cr(VI) solution was prepared by dissolving an amount of $K_2Cr_2O_7$ in the deionized water (100 mL solution for each experiment, and the concentration of Cr(VI) was 1000 mg/L).Then, the prepared biochar was added into the beaker as the solution was heated to a predetermined temperature. After a required reaction time, the solution with Cr (III) and retained biochar were separated by vacuum filtration. The concentration of Cr (VI) in the filtrate was determined by titration with ferrous ammonium sulfate [12,13,21], and the reduction efficiency (η) of Cr (VI) was calculated following Equation (1):

$$\eta = \frac{C_0 - C_t}{C_0} \times 100\% \quad (1)$$

where C_0 is the initial concentration of Cr (VI) in the solution, mg/L; C_t, is the concentration of Cr (VI) in the solution at a reaction time of t, mg/L.

2.3. Response Surface Optimization

The interactions between the experimental parameters were important for the experimental results, which were ignored during the single-factor experiment; thus, RSM was applied to optimize the experimental process and order the significance of the experimental parameters [13,29,30]. In this paper, the experimental parameters that affected the reduction process were selected as A (m (C)/m(Cr)), B (reaction temperature), C (reaction time), and D (concentration of H_2SO_4). The actual values for them were confirmed through the single-factor experimental results and displayed in Table 1.

Table 1. Independent variables and factor levels.

Independent Variable	Unit	Level		
		−1	0	1
A:m(C)/m(Cr)	-	0.5	1.75	3.0
B: Reaction temperature	°C	30	60	90
C: Reaction time	min	10	35	60
D: Concentration of H_2SO_4	g/L	0	10	20

3. Results and Discussion

The dosage of biochar had a significant effect on the reduction of Cr (VI), as it was the main reaction reagent. A series of experiments were conducted to investigate the effect of the dosage of biochar (m(C)/m(Cr)) on the reduction efficiency of Cr (VI). The m(C)/m(Cr) was set as m(C)/m(Cr) = 0.5, 1.0, 1.5, 2.0, 2.5, and 3.0. The other reaction conditions were kept as constant: Reaction temperature of 90°C, reaction time of 60 min, and concentration of H_2SO_4 at 10 g/L. The results shown in Figure 1a indicate that the reduction efficiency of Cr (VI) increased with an increase in m(C)/m(Cr). The reduction efficiency of Cr (VI) increased from 40.32% to 97.74% as the dosage of biochar increased from m(C)/m(Cr) = 0.5 to m(C)/m(Cr) = 3.0. Thus, m(C)/m(Cr) =3.0 was selected for further experiments.

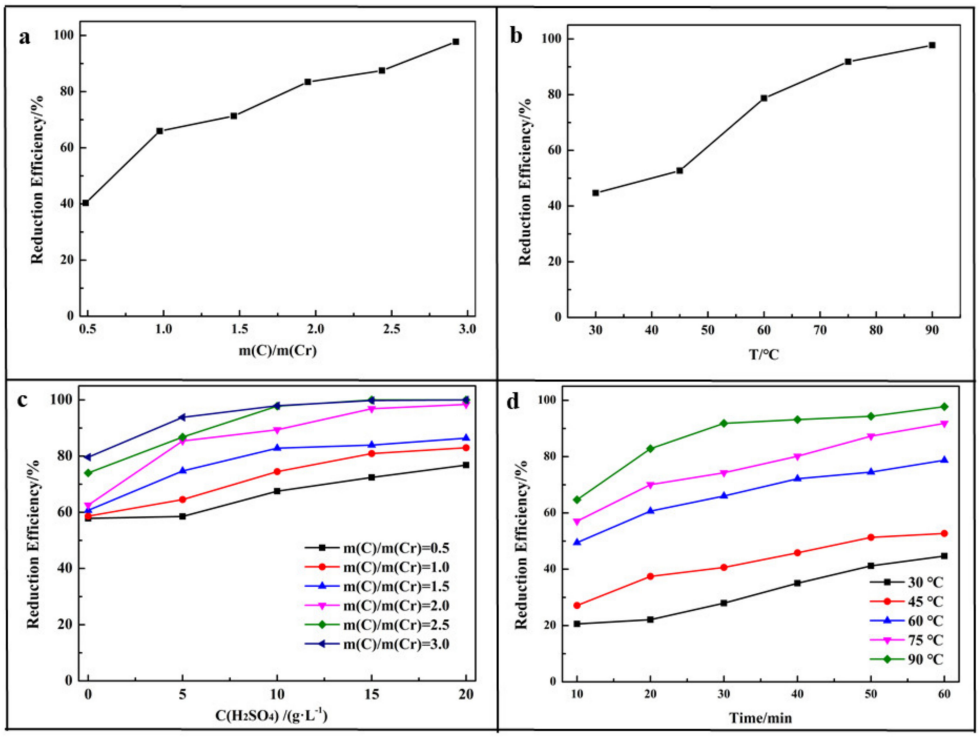

Figure 1. Effect of the single parameters on the reduction process: (**a**) Dosage of biochar (m(C)/m(Cr)); (**b**) reaction temperature; (**c**) concentration of H2SO4; (**d**) reaction time.

The reaction temperature plays an important role in a standard chemical reaction. A series of experiments were conducted to investigate the effect of the reaction temperature on the reduction efficiency of Cr (VI), and the reaction temperature was set as 30, 45, 60, 75, and 90 °C. The other reaction conditions were kept constant: m(C)/m(Cr) = 3.0, reaction time of 60 min, and concentration of H_2SO_4 at 10 g/L. It can be seen from Figure 1b that the reduction efficiency increased with an increase in the reaction temperature, and the increasing trend of the reduction efficiency was similar to the dosage of biochar, which indicates that both the dosage of biochar and the reaction temperature have a significant

effect on the reduction process. A higher temperature can intensify the activity of biochar molecules and Cr (VI) ions, promote the extent of the reduction reaction, and enforce the reduction of Cr (VI) [12,13,31]. Therefore, 90 °C was selected as the optimal reaction temperature for further experiments.

A recent study indicated that Cr (VI) is easily reduced to Cr (III) in a strong acidic medium [12,13,21]. A series of experiments were conducted with the concentration of H_2SO_4 ranging from 0 to 20 g/L at various dosages of biochar. Figure 1c shows that an increase in the concentration of H_2SO_4 could facilitate the reduction process of Cr (VI). In theory, the formation of $HCrO_4^-$ is the main species of Cr (VI) at 0.8 < pH < 6.8, and CrO_4^{2-} is the main species at pH > 6.8 (Figure 2a, measured by software Visual MINTEQ [32]). In contrast, $HCrO_4^-$ is more easily reduced into Cr (III) than CrO_4^{2-}, as the oxidation potential of $HCrO_4^-$ was higher according to the results shown in Figure 2b ($E0(HCrO_4^-/Cr^{3+})$ = 1.35 V, $E0(CrO_4^{2-}/Cr^{3+})$ = 0.56 V). When the dosage of biochar was much higher, the reduction efficiency experienced no obvious increase (when m(C)/m(Cr) was up to 2.5, the reduction efficiency of Cr (VI) was nearly 100% at 10 g/L). Thus, the concentration of H_2SO_4 at 10 g/L was enough for further experiments.

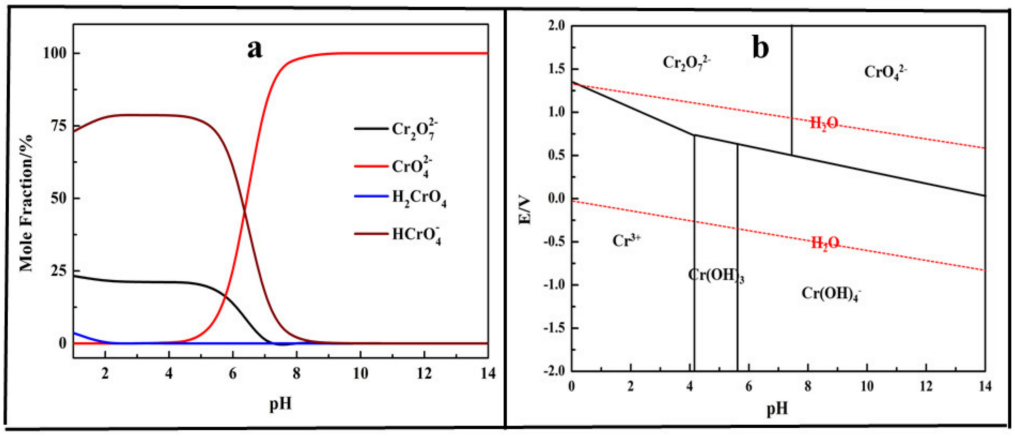

Figure 2. (**a**) Cr (VI) species in the solution at various pH levels; (**b**) E-pH diagram of chromium.

Figure 1d describes the effect of the reaction time on the reduction process at various reaction temperatures, with the other reaction conditions kept as m(C)/m(Cr) = 3.0 and a concentration of H_2SO_4 at 10 g/L. The results showed that extending the reaction time could improve the reduction efficiency of Cr (VI) at all reaction temperatures. Additionally, a higher reaction temperature was beneficial for the reduction process, which is consistent with the analysis above.

3.1. Response Surface Methodology

3.1.1. Model Fitting

The square root was used to express the simulated results, presented in Equation (2):

$$\text{sqrt}(\eta) = 8.38 + 0.55*A + 0.38*B + 0.27*C + 0.52*D - 0.17*AB + 0.22*AC + 0.25*AD - 0.025*BC + 0.25*BD + 0.20*CD - 0.03*A2 + 0.25*B2 + 0.02*C2 - 0.30*D2 \quad (2)$$

The influence of each parameter on the reduction efficiency of Cr (VI) can be seen from the coefficients before them in Equation (2). The coefficients of each parameter were 0.55, 0.38, 0.27 and 0.52, respectively, confirming that all of the parameters had a positive effect on the reduction efficiency. The results displayed in Figure 3 indicate that the influence of each parameter on the reduction efficiency followed the order: A> D > B > C, which is consistent with the results described in Equation (2). Above all, the dosage of biochar and the concentration of H_2SO_4 had the greatest influence on the reduction process.

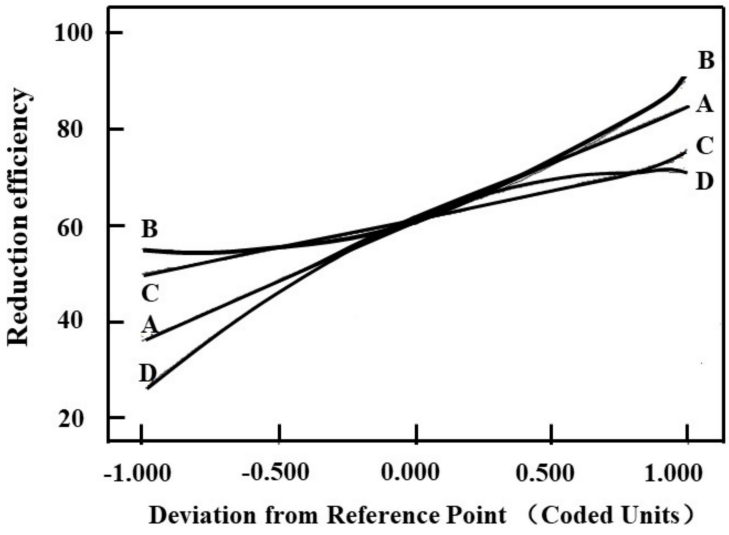

Figure 3. Perturbation plot for the reduction efficiency of Cr (VI) in the design space: (**A**) m (C)/m(Cr); (**B**) reaction temperature; (**C**) reaction time; (**D**) concentration of H_2SO_4.

The analysis of variance of the reduction efficiency of Cr (VI) is shown in Table 2. The results show that the *p*-value of the model was <0.0001, which indicates that the selected model was significant and suitable for simulating the reduction process of Cr (VI) [21,30]

Table 2. Analysis of variance for the response.

Source	Sum of Squares	Z	Mean Square	F Value	*p*-Value Prob > F
Model	11.76	14	0.84	14.47	<0.0001
A	3.60	1	3.60	62.00	<0.0001
B	1.76	1	1.76	30.29	<0.0001
C	0.87	1	0.87	15.05	0.0017
D	3.31	1	3.31	56.94	<0.0001
AB	0.12	1	0.12	2.10	0.1690
AC	0.19	1	0.19	3.36	0.0882
AD	0.24	1	0.24	4.22	0.0591
BC	0.00254	1	0.00254	0.044	0.8372
BD	0.26	1	0.26	4.39	0.0547
CD	0.16	1	0.16	2.67	0.1243
A^2	0.005787	1	0.005787	0.100	0.7569
B^2	0.41	1	0.41	7.05	0.0188
C^2	0.002533	1	0.002533	0.044	0.8375
D^2	0.60	1	0.60	10.32	0.0063
Residual	0.81	14	0.058	-	-
Lack-of-fit	0.81	10	0.081	-	-
Pure error	0.000	4	0.000	-	-

3.1.2. Response Surface Analysis

To evaluate the fitting effect of the model on the experimental results, some other important diagnostic plots, including internally studentized residuals against run number, predicted against actual, internally studentized residuals against predicted, and normal probability against internally studentized residuals, are shown in Figure 4. All points shown in the normal probability against internally studentized residuals plot shown in Figure 4a are concentrated in a straight line, illustrating that the error was normally distributed. In a plot of internally studentized residuals against run number and internally studentized residuals against predicted, the residuals were randomly distributed between +3.00 and −3.00, indicating that the Box–Behnken model successfully established the

relationship between the independent variable and the reduction efficiency. A plot of predicted against actual is shown in Figure 4b; the points are approximately distributed on a straight line with a slope of 1, which indicates that this model accurately predicted the actual value.

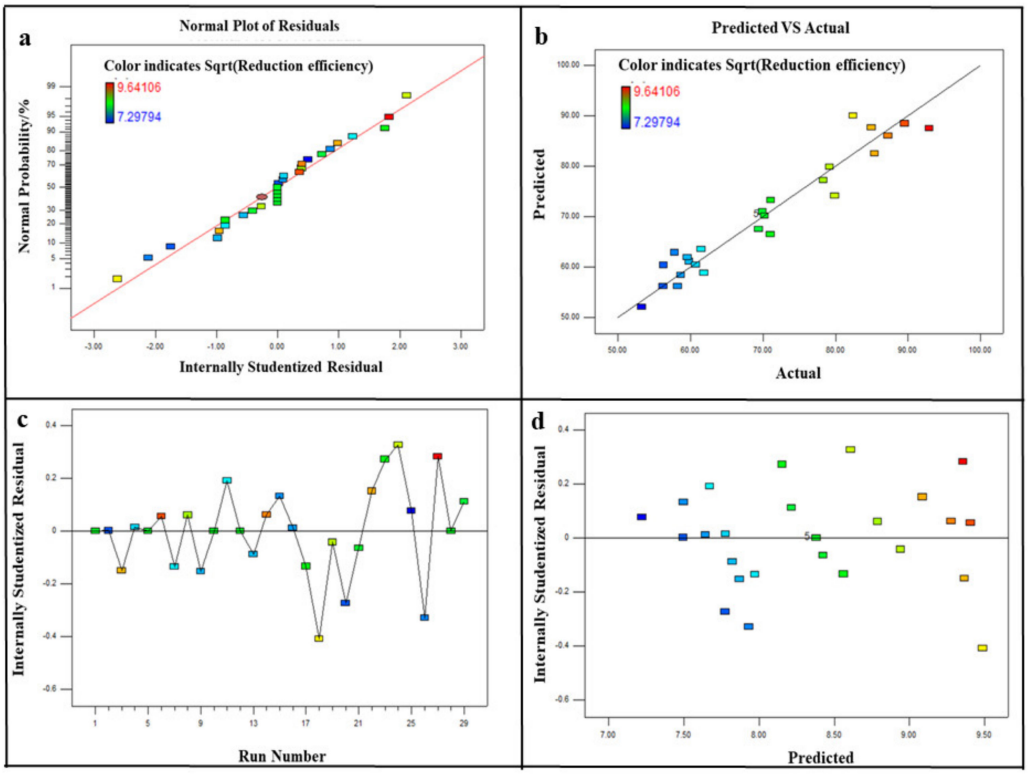

Figure 4. Diagnostic plots of the quadratic model: (**a**) Normal probability against internally studentized residuals; (**b**) predicted against actual; (**c**) internally studentized residuals against run number; (**d**) internally studentized residuals against predicted.

The contour plots were applied to analyze the interaction between the experimental parameters. According to the contour plots, the degree of influence of the experimental factors could be judged. As far as the influence of the individual experimental factor is concerned, the four factors all had great effects on the reduction efficiency. It is clear that the reduction efficiency increased with the dosage of biochar (m(C)/m(Cr)) according to the results shown in Figure 5. Though the four factors all had a positive influence on the reduction process of Cr (VI), the interaction of the dosage of biochar and the reaction temperature, as well as the reaction temperature and the reaction time, had a negative influence on the reduction process. The results are consistent with the analysis above.

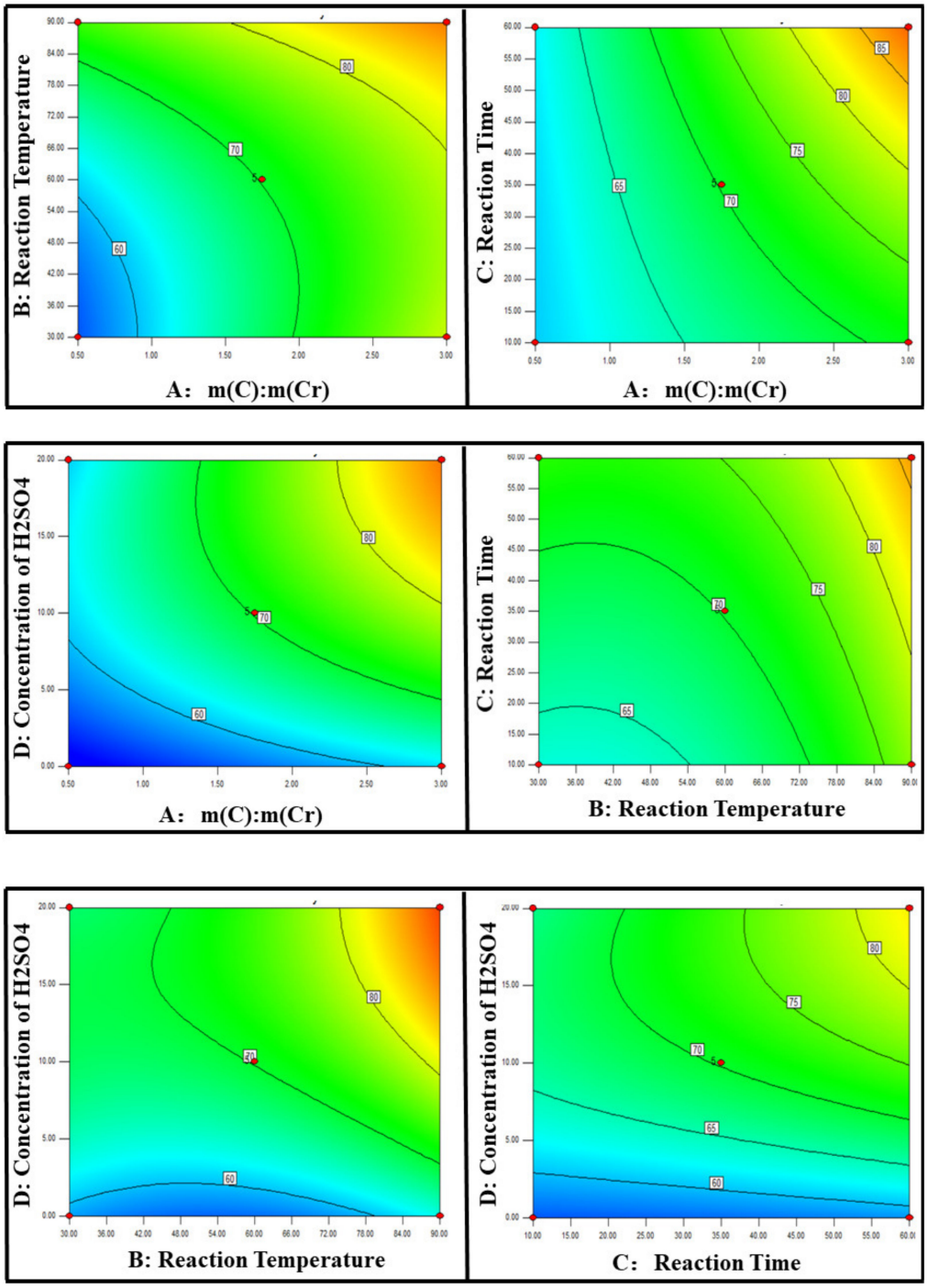

Figure 5. Response surface plots for the factors.

3.2. Reduction Kinetics Analysis

In this paper, the pseudo-first-order model—as described as Equation (3)—was applied to simulate the reduction behavior of Cr (VI) [12,21,33,34].

$$\upsilon = dC/dt = -KC \quad (3)$$

Integrate.

$$-LnC = Kt - Ln\,C_0 \quad (4)$$

where v is the reduction rate of Cr (VI); C is the concentration of Cr (VI); C_0 is the initial concentration of Cr (VI); K is the reduction reaction constant.

Figure 6a displays the results of the experimental results fitted with Equation (4), which indicates that the reduction process of Cr (VI) was fitted well with the pseudo-first-order model. The reduction reaction's apparent activation energy was obtained by simulating the experimental results with the Arrhenius Equation (Equation (5)). The apparent activation energy was calculated as 40.24 kJ/mol according to the results showed in Figure 6b, which was much larger than the apparent energy calculated for reduction with oxalic acid (22.49 kJ/mol) [21] and electrochemical reduction (4.74 kJ/mol) [12]. This means that the reduction process with biochar was harder than oxalic acid and electrochemical reduction.

$$\ln K = \mathrm{Ln}A - Ea/RT \quad (5)$$

where Ea is the apparent activation energy; A is the pre-exponential factor; R is the molar gas constant, 8.314 J/(mol K); K is the reduction reaction constant at different reaction temperatures.

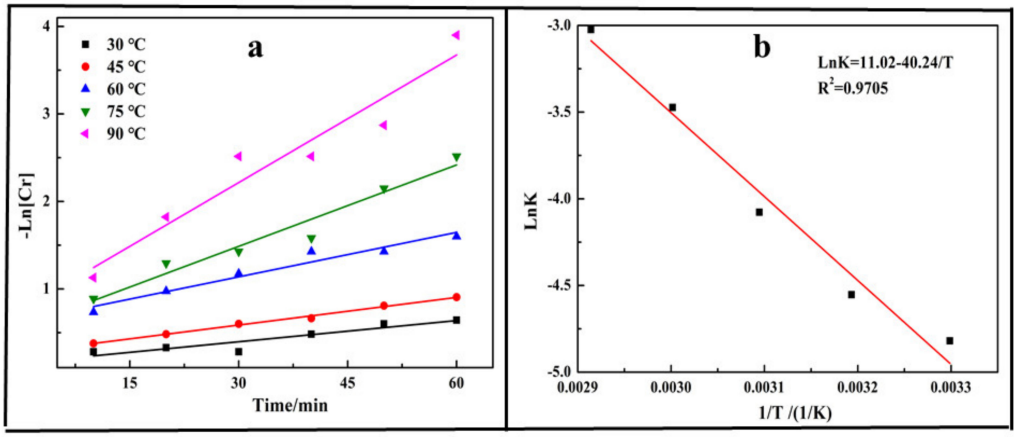

Figure 6. Kinetics plots: (**a**) Plot of reduction kinetics at various reaction temperatures; (**b**) natural logarithm of the reduction reaction constant vs. the reciprocal reaction temperature.

3.3. Removal of Chromium (III)

After the reduction process, Cr (VI) was reduced to Cr (III) and it was removed by precipitation with sodium hydroxide [35] or adsorption with melamine [19,20].

4. Conclusions

Cr (VI) in wastewater is a serious problem and urgently needs treating. In this paper, a highly efficient reduction process of Cr (VI) with biochar was investigated, while it was thought to be an adsorption process in our first purpose, and the following conclusions could be obtained:

(1) Cr (VI) was easily reduced by biochar at a high reaction temperature with a high dosage of biochar in a strong acidic medium. Nearly 100% of Cr (VI) was reduced at the selected reaction conditions: Dosage of biochar at m (C)/m(Cr) = 3.0, reaction temperature of 90 °C, reaction time of 60 min, and concentration of H_2SO_4 of 20 g/L.

(2) The reduction kinetics analysis indicated that the reduction behavior of Cr (VI)with biochar fitted well with the pseudo-first-order model, and the apparent activation energy was calculated as 40.24 kJ/mol, which was much larger than the apparent energy calculated for reduction with oxalic acid (22.49 kJ/mol) and electrochemical reduction (4.74 kJ/mol).

(3) Response surface methodology confirmed that all of the experimental parameters had a positive effect on the reduction of Cr (VI). The influence of each factor on the reduction process followed the order: A (dosage of biochar (m (C)/m(Cr)) > D (concentration of H_2SO_4) > B (reaction temperature) > C (reaction time). In particular,

the dosage of biochar and the concentration of H_2SO_4 had the greatest influence on the reduction process.

Author Contributions: Conceptualization, H.P.; methodology, H.P.; software, H.P.; validation, H.P.; formal analysis, H.P.; investigation, H.Q., C.W., and J.G.; resources, H.P.; data curation, Z.H., C.Z., Y.G., Y.R., and J.G.; writing—original draft preparation, H.P.; writing—review and editing, H.P.; visualization, H.P.; supervision, H.P.; project administration, H.P.; funding acquisition, H.P. All authors have read and agreed to the published version of the manuscript.

Funding: This work was supported by the Science and Technology Research Program of the Chongqing Municipal Education Commission (No. KJQN201901403 and No. CXQT20026) and the Chongqing Science and Technology Commission (No. cstc2018jcyjAX0018).

Institutional Review Board Statement: Not applicable.

Informed Consent Statement: Not applicable.

Data Availability Statement: All the data were included in this paper.

Conflicts of Interest: The authors declare no conflict of interest.

References

1. Song, J.; Kong, H.; Jang, J. Adsorption of heavy metal ions from aqueous solution by polyrhodanine-encapsulated magnetic nanoparticles. *J. Colloid. Interf. Sci.* **2011**, *359*, 505–511. [CrossRef] [PubMed]
2. Kyzas, G.Z.; Matis, K.A. Nanoadsorbents for pollutants removal: A review. *J. Mol. Liq.* **2015**, *203*, 159–168. [CrossRef]
3. Nogueira, V.; Lopes, I.; Rocha-Santos, T.; Gonçalves, F.; Pereira, R. Toxicity of solid residues resulting from wastewater treatment with nanomaterials. *Aquat. Toxicol.* **2015**, *165*, 172–178. [CrossRef] [PubMed]
4. Adhoum, N.; Monser, L.; Bellakhal, N.; Belgaied, J.-E. Treatment of electroplating wastewater containing Cu^{2+}, Zn^{2+} and Cr(VI) by electrocoagulation. *J. Hazard. Mater.* **2004**, *112*, 207–213. [CrossRef]
5. Hunsom, M.; Pruksathorn, K.; Damronglerd, S.; Vergnes, H.; Duverneuil, P. Electrochemical treatment of heavy metals (Cu^{2+}, Cr^{6+}, Ni^{2+}) from industrial effluent and modeling of copper reduction. *Water Res.* **2005**, *39*, 610–616. [CrossRef]
6. Peng, H.; Guo, J. Removal of chromium from wastewater by membrane filtration, chemical precipitation, ion exchange, adsorption electrocoagulation, electrochemical reduction, electrodialysis, electrodeionization, photocatalysis and nanotechnology: Review. *Environ. Chem. Lett.* **2021**, *19*, 1383–1393. [CrossRef]
7. Azimi, A.; Azari, A.; Rezakazemi, M. Ansarpour, Removal of Heavy Metals from Industrial Wastewaters: A Review. *ChemBioEng Rev.* **2017**, *4*, 37–59.
8. Xin, H.; Xinhong, Q.; Jinyi, C. Preparation of Fe(II)–Al layered double hydroxides: Application to the adsorption/reduction of chromium. *Colloids Surf. A Physicochem. Eng. Asp.* **2017**, *516*, 362–374.
9. Fu, R.; Zhang, X.; Xu, Z.; Guo, X.; Bi, D.; Zhang, W. Fast and highly efficient removal of chromium (VI) using humus-supported nanoscale zero-valent iron: Influencing factors, kinetics and mechanism. *Sep. Purif. Technol.* **2017**, *174*, 362–371. [CrossRef]
10. Peng, H.; Guo, J.; Li, B.; Liu, Z.; Tao, C. High-efficient recovery of chromium (VI) with lead sulfate. *J. Taiwan Inst. Chem. Eng.* **2018**, *85*, 149–154. [CrossRef]
11. Zhao, Y. Removal of Chromium Using Electrochemical Approaches: A Review. *Int. J. Electrochem. Sci.* **2018**, *13*, 1250–1259. [CrossRef]
12. Peng, H.; Leng, Y.; Guo, J. Electrochemical Removal of Chromium (VI) from Wastewater. *Appl. Sci.* **2019**, *9*, 1156. [CrossRef]
13. Peng, H.; Leng, Y.; Cheng, Q.; Shang, Q.; Shu, J.; Guo, J. Efficient Removal of Hexavalent Chromium from Wastewater with Electro-Reduction. *Processes* **2019**, *7*, 41. [CrossRef]
14. Zhao, Z.; He, A.; Lin, J.; Feng, M.; Murugadoss, V.; Ding, T.; Liu, H.; Shao, Q.; Mai, X.; Wang, N.; et al. Progress on the Photocatalytic Reduction Removal of Chromium Contamination. *Chem. Rec.* **2019**, *19*, 873–882. [CrossRef] [PubMed]
15. Zheng, X.; Kang, F.; Liu, X.; Peng, H.; JinYang, Z. Carbon-coated Mg–Al layered double oxide nanosheets with enhanced removal of hexavalent chromium. *J. Ind. Eng. Chem.* **2019**, *80*, 53–64. [CrossRef]
16. Liu, X.Q.; Zhang, G.; Xing, H.Q.; Huang, P.; Zhang, X.L. Preparation of amphiphilic composite and removal of oil and hexavalent chromium from wastewater. *Environ. Chem. Lett.* **2011**, *9*, 127–132. [CrossRef]
17. He, C.; Gu, L.; Xu, Z.; He, H.; Fu, G.; Han, F.; Huang, B.; Pan, X. Cleaning chromium pollution in aquatic environments by bioremediation, photocatalytic remediation, electrochemical remediation and coupled remediation systems. *Environ. Chem. Lett.* **2020**, *18*, 561–576. [CrossRef]
18. Gallios, G.P.; Vaclavikova, M. Removal of chromium (VI) from water streams: A thermodynamic study. *Environ. Chem. Lett.* **2008**, *6*, 235–240. [CrossRef]
19. Peng, H.; Shang, Q.; Chen, R.; Zhang, L.; Chen, Y.; Guo, J. Step-Adsorption of Vanadium (V) and Chromium (VI) in the Leaching Solution with Melamine. *Sci. Rep.* **2020**, *10*, 6326. [CrossRef]

20. Guo, J.; Chen, R.; Zhang, L.; Shang, Q.; Chen, Y.; Peng, H. Adsorption of Chromium (III) on Melamine: Kinetic, Isotherm, Thermodynamics and Mechanism Analysis. *IOP Conf. Ser. Earth Environ. Sci.* **2020**, *512*, 012076. [CrossRef]
21. Peng, H.; Guo, J. Reduction behavior of chromium(VI) with oxalic acid in aqueous solution. *Sci. Rep.* **2020**, *10*, 17732. [CrossRef]
22. Ashiq, A.; Sarkar, B.; Adassooriya, N.; Walpita, J.; Rajapaksha, A.U.; Ok, Y.S.; Vithanage, M. Sorption process of municipal solid waste biochar-montmorillonite composite for ciprofloxacin removal in aqueous media. *Chemosphere* **2019**, *236*, 124384. [CrossRef] [PubMed]
23. Huang, W.-H.; Lee, D.-J.; Huang, C. Modification on biochars for applications: A research update. *Bioresour. Technol.* **2021**, *319*, 124100. [CrossRef] [PubMed]
24. Zheng, X.; Zhou, Y.; Liu, X.; Fu, X.; Peng, H.; Lv, S. Enhanced adsorption capacity of MgO/N-doped active carbon derived from sugarcane bagasse. *Bioresour. Technol.* **2020**, *297*, 122413. [CrossRef]
25. Ahmed, M.B.; Zhou, J.L.; Ngo, H.H.; Guo, W.; Johir, M.A.H.; Belhaj, D. Competitive sorption affinity of sulfonamides and chloramphenicol antibiotics toward functionalized biochar for water and wastewater treatment. *Bioresour. Technol.* **2017**, *238*, 306–312. [CrossRef] [PubMed]
26. Karri, R.R.; Sahu, J.N.; Meikap, B.C. Improving efficacy of Cr (VI) adsorption process on sustainable adsorbent derived from waste biomass (sugarcane bagasse) with help of ant colony optimization. *Ind. Crop. Prod.* **2020**, *143*, 111927. [CrossRef]
27. Zubair, M.; Ihsanullah, I.; Aziz, H.A.; Ahmad, M.A.; Al-Harthi, M.A. Sustainable wastewater treatment by biochar/layered double hydroxide composites: Progress, challenges, and outlook. *Bioresour. Technol* **2021**, *319*, 124128. [CrossRef] [PubMed]
28. Peng, H.; Yang, L.; Wang, L.; Guo, J.; Li, B. Recovery of vanadium with urea in acidic medium. *Environ. Chem. Lett.* **2019**, *17*, 1867–1871. [CrossRef]
29. Peng, H.; Shang, Q.; Chen, R.; Leng, Y.; Guo, J.; Liu, Z.; Tao, C. Oxidative Leaching Kinetics of Vanadium from the Vanadium-Chromium-Reducing Residue with $K_2Cr_2O_7$. *ACS Omega* **2020**, *5*, 8777–8783. [CrossRef]
30. Peng, H.; Wang, F.; Li, G.; Guo, J.; Li, B. Highly Efficient Recovery of Vanadium and Chromium: Optimized by Response Surface Methodology. *ACS Omega* **2019**, *4*, 904–910. [CrossRef]
31. Peng, H.; Yang, L.; Chen, Y.; Guo, J.; Li, B. Recovery and Separation of Vanadium and Chromium by Two-Step Alkaline Leaching Enhanced with Electric Field and H_2O_2. *ACS Omega* **2020**, *5*, 5340–5345. [CrossRef] [PubMed]
32. Gustafsson, J.P. Visual MINTEQ ver. 3.0. 2014.
33. Chen, G.; Han, J.; Mu, Y.; Yu, H.; Qin, L. Two-stage chromium isotope fractionation during microbial Cr(VI) reduction. *Water Res.* **2019**, *148*, 10–18. [CrossRef] [PubMed]
34. Okello, V.A.; Mwilu, S.; Noah, N.; Zhou, A.; Chong, J.; Knipfing, M.T.; Doetschman, D.; Sadik, O.A. Reduction of hexavalent chromium using naturally-derived flavonoids. *Environ. Sci. Technol.* **2014**, *46*, 10743–10751. [CrossRef] [PubMed]
35. Chen, B.; Huang, S.; Liu, B.; Ge, Q.; Wang, M.; Wang, X. Separation and recovery of vanadium and chromium from acidic leach solution of V-Cr-bearing reducing slag. *J. Environ. Chem. Eng.* **2017**, *5*, 4702–4706. [CrossRef]